

RSC Advances



This is an *Accepted Manuscript*, which has been through the Royal Society of Chemistry peer review process and has been accepted for publication.

Accepted Manuscripts are published online shortly after acceptance, before technical editing, formatting and proof reading. Using this free service, authors can make their results available to the community, in citable form, before we publish the edited article. This *Accepted Manuscript* will be replaced by the edited, formatted and paginated article as soon as this is available.

You can find more information about *Accepted Manuscripts* in the [Information for Authors](#).

Please note that technical editing may introduce minor changes to the text and/or graphics, which may alter content. The journal's standard [Terms & Conditions](#) and the [Ethical guidelines](#) still apply. In no event shall the Royal Society of Chemistry be held responsible for any errors or omissions in this *Accepted Manuscript* or any consequences arising from the use of any information it contains.

Graphical Abstract

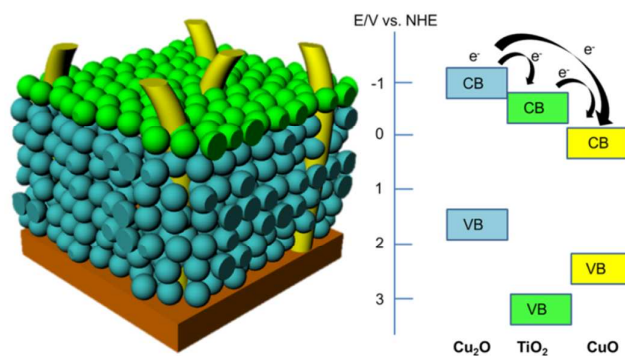
Introducing a Protective Interlayer of TiO₂ in Cu₂O-CuO Heterojunction Thin Film as a Highly Stable Visible Light Photocathode

Peng Wang^a, Xiaoming Wen^b, Rose Amal^{*a} and Yun Hau Ng^{*a}

^aParticles and Catalysis Research Group, School of Chemical Engineering, The University of New South Wales, Sydney NSW 2052, Australia.

^bSchool of Photovoltaics and Renewable Energy Engineering, The University of New South Wales, Sydney NSW 2052, Australia.

Corresponding author: Y. H. Ng (yh.ng@unsw.edu.au), R. Amal (r.amal@unsw.edu.au)



Photoactivity and stability of Cu₂O-CuO heterojunction thin films are enhanced by incorporating an interlayer of TiO₂ to minimise the redox reactions at Cu₂O-electrolyte interface. High visible light-induced current generation is observed due to the well-matched band gap structure alignment, where TiO₂ layer facilitates charge transfer from Cu₂O to CuO thermodynamically, minimising the possible loss of electron-hole recombination.

ARTICLE

Introducing a Protective Interlayer of TiO₂ in Cu₂O-CuO Heterojunction Thin Film as a Highly Stable Visible Light Photocathode

Cite this: DOI: 10.1039/x0xx00000x

Peng Wang^a, Xiaoming Wen^b, Rose Amal^{*a} and Yun Hau Ng^{*a}

Received 00th January 2012,
Accepted 00th January 2012

DOI: 10.1039/x0xx00000x

www.rsc.org/

Visible light-induced photocurrent generation and photoelectrochemical stability of p-type Cu₂O-CuO photocathodes are improved significantly upon incorporating an interlayer of TiO₂ between Cu₂O and CuO. The TiO₂ layer hinders the electron conduction at the semiconductor-electrolyte interface (improved stability) as well as promotes electron transfer from Cu₂O to CuO (increased photocurrent). Upon visible light illumination, the optimised multilayer Cu₂O-TiO₂-CuO heterojunction thin film yields photocurrent of 2.4 mA/cm² and retains 75% of its photoactivity over the measurement period. By comparison, the unmodified Cu₂O-CuO generates photocurrent of 1.3 mA/cm² with photoactivity retention of only 32% after prolonged illumination. Wavelength-dependent incident photon-to-current efficiency (IPCE) reveals a considerable enhancement over the excitation region of Cu₂O (400 – 560 nm). Transient fluorescence decay analysis suggests the promotion of electron transfer from Cu₂O to CuO through TiO₂. As a result, both photoactivity and photochemical stability of the photocathodes are improved.

Introduction

Splitting water into its elemental components, i.e. H₂ and O₂, is regarded as the cleanest and the most sustainable way to meet energy demands while addressing stringent environmental concerns. Even though traditional electrolysis of water has been known for decades,^[1] currently water splitting triggered by sunlight is attracting attention of the research community as all energy input, conversion and output occur in clean and renewable forms.^[2] Since the discovery of photoelectrochemical (PEC) water splitting using UV-illuminated TiO₂ electrodes by Honda and Fujishima,^[3] extensive work has been carried out to develop an efficient PEC water splitting system. Various photoactive electrodes have been made and investigated with the majority of the examples based on n-type semiconductors (e.g. WO₃,^[4] BiVO₄^[5] and GaInP₂^[6]). Electrons photogenerated in n-type semiconductors, with the aide of external voltage supplied, can be transported to the counter electrode (mostly platinum (Pt)) to reduce water. A p-type photoactive semiconductor is the ideal candidate to replace Pt for use in a “tandem” configuration which excludes or minimises the supply of external energy to split water in a photoelectrochemical process.^[7, 8] However, few examples of highly efficient p-type semiconductors have been reported so far.

p-type Cu₂O has distinguished itself by its abundance, low-cost and, more impressively, its high theoretical photocurrent of -14.7 mA/cm².^[9-11] It has a suitable direct optical band gap of 2 – 2.2 eV ($\lambda < 560$ nm in the visible light range), where the conduction band (CB) is 0.7 V more negative than the reduction potential of water and the valence band (VB) is just more positive than the oxidation potential of water.^[9, 10] Electrons excited into CB of Cu₂O are sufficiently energetic to be transferred to water for H₂ production. Despite all these advantages, the Cu₂O photoelectrode is chemically unstable due to a self-photodegradation mechanism. As the redox potential of Cu₂O lies between its CB and VB, it can either be self-reduced (Cu₂O to Cu) or self-oxidised (Cu₂O to CuO) by the photogenerated electrons or holes, respectively, upon visible light illumination.^[12] Thimsen and co-workers introduced an ultra-thin protective layer of ZnO:Al/TiO₂ on top of the Cu₂O photoelectrode using atomic layer deposition (ALD).^[12] The ZnO:Al/TiO₂ layer protected Cu₂O from direct electron conduction with the electrolyte interface. Instead, it allowed the electrons to flow from Cu₂O to the electrolyte through the protective layer. This strategy greatly suppressed the photodegradation of Cu₂O. It has been adopted for surface passivation of other p-type photocathodes including Si-photoelectrode to extend the lifetime of p-type semiconductors in a solid-liquid junction cell.^[13, 14] Nonetheless, ALD treatment

of thin film requires costly instrumentation and large-scale treatment is challenging. Wang's group subsequently introduced a thin CuO layer with a function similar to the previously elaborated ZnO:Al/TiO₂ on Cu₂O photoelectrode by using a combination of electrodeposition, anodisation and calcination.^[15] The CuO top layer was found to reduce the photocorrosion of Cu₂O as well as the charge recombination rate during water splitting reaction.

We recently developed an anodised Cu₂O thin film with the surface decorated with CuO nanowires grown from the Cu₂O layer underneath.^[16] The embedment of these CuO nanowires derived from thermal treatment was found to improve the adhesion of Cu₂O layers to the substrate. The enhanced mechanical stability together with the partial surface passivation towards the Cu₂O-electrolyte interface contributed to an improved PEC stability of the film. In this work, adopting the working principle of surface passivation, by using a dip-coating technique we introduce an interlayer of anatase TiO₂ in between the Cu₂O under layer and CuO top layer. Dip-coating is a fast, simple and, more importantly, scalable method of large film treatment. The introduction of TiO₂ interlayer offers a number of advantages to improve the PEC performance of the Cu₂O photocathode. Firstly, it minimises the direct electron conduction between Cu₂O and electrolyte, which usually leads to the photocorrosion of Cu₂O. Secondly, a thin layer of TiO₂ does not affect the penetration of visible light to reach Cu₂O underneath; therefore, comparable light absorption in Cu₂O could be expected. Thirdly, the strategic alignment of the band gap structure among Cu₂O, TiO₂ and CuO can promote an efficient electron transfer pathway for higher electron consumption efficiency. As a result, both photocurrent generation and retention of photoactivity in our new photoelectrodes were greatly improved. A thorough investigation on the origin of the enhancement was performed and the electron transfer kinetics between the tri-components was studied.

Experimental section

Preparation of unmodified and TiO₂-modified Cu₂O-CuO photoelectrodes

All chemicals used in these studies were of analytical grade without further purification. The Cu foil (99.9%, Aldrich) was sonicated first in ethanol/ acetone solution (1:1), followed by Milli-Q water for 10 min each. A two-electrode, in-house designed anodisation cell was used, with Cu foil as the working electrode and platinum plate and wire as the counter electrode. Cu₂O was synthesised by anodising the Cu foil in an alkaline electrolyte at 10 V for 10 min by a programmable DC power supply (PST-3201, GW Instek). The alkaline electrolyte was composed of 96.05 wt% of ethylene glycol (>99%, Aldrich), 0.75 wt% of potassium hydroxide (>99%, Aldrich) and 3.0 wt% of water with 0.20 wt% sodium fluoride (>99%, Aldrich). After anodisation, the prepared Cu₂O foil was washed with Milli-Q water to remove unwanted debris or precipitates and dried under ambient air for 1 h. The unmodified Cu₂O-CuO

photoelectrode was fabricated by calcination of the anodised Cu₂O thin film at 400 °C for 1 h. The TiO₂-modified Cu₂O-CuO photoelectrode was synthesised by dip-coating to create a TiO₂ interlayer between the Cu₂O under layer and CuO top layer. A pre-determined optimised 2.0 M titanium isopropoxide solution in ethanol was used as the TiO₂ precursor. The dip-coating procedure on the anodised Cu₂O foil was carried out for 30 min. In order to investigate the influence of TiO₂ coverage on Cu₂O-CuO photoelectrodes, Cu₂O-CuO photoelectrodes modified with 2.0 M TiO₂ precursor at different duration ranging from 10 min to 60 min were also prepared. After dip-coating of TiO₂ precursor, the foils were annealed in air at identical conditions.

Material characterization

The morphology and nanostructure of unmodified Cu₂O-CuO and TiO₂-modified Cu₂O-CuO photoelectrodes were analysed by scanning electron microscopy (SEM, S900, Hitachi). The phase and crystallinity of the thin film were investigated by X-ray diffraction (XRD, X'pert Pro MRD, Philips, using Cu K α radiation $\lambda = 1.54\text{\AA}$). The distribution of TiO₂ particles on the layer of Cu₂O was detected by energy dispersive spectrometry (EDS, NanoSEM 230, FEI Nova). The surface chemical composition was characterized by X-ray photoemission spectrometry (XPS, ESCALAB220i-XL, Thermo Scientific) with Al K α at 1486.6 eV. All the XPS data were calibrated to the carbon 1s peak at 285 eV. Fluorescence lifetimes were measured using the time correlated single photon counting (TCSPC) technique on a Microtime-200 system (Picoquant) with an excitation by a 405 nm laser. The system has time resolution of about 200 ps.

Photoelectrochemical performance

Photoelectrochemical characterization was carried out using a standard three-electrode electrochemical cell, which has a quartz window for light penetration and a hole for clamping samples. Platinum wire was used as the counter electrode and an Ag/AgCl electrode was employed as the reference electrode. The electrolyte used for all PEC measurements was a 0.5 M K₂SO₄ solution purged with argon to remove dissolved air. The photoelectrochemical properties including photocurrent density and photocurrent transient responses were recorded with a potentiostat (PG STAT-302N, Autolab) under on-off illumination cycles. The illumination source was a 300 W xenon arc lamp (PLS-SXE300) equipped with cut-off filter at 420 nm. Incident photon-to-current efficiency (IPCE) was measured using a 280 W xenon lamp (Newport 66902) coupled with a monochromator (Newport 74125).

Results and discussion

Fig. 1a and **b** show the surface morphology of unmodified Cu₂O-CuO and TiO₂-modified Cu₂O-CuO photoelectrodes. As described in our earlier work using high resolution transmission electron microscopy,^[16] the unmodified Cu₂O-CuO photoelectrode comprises two distinct component layers, i.e. a

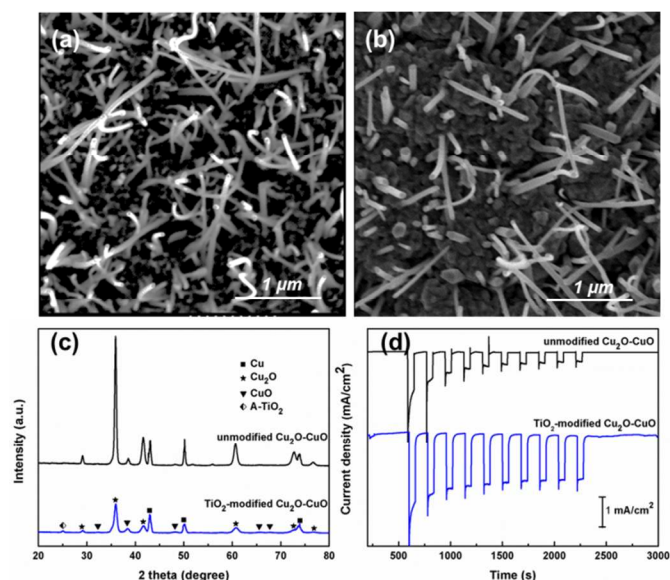


Fig. 1 SEM images of (a) unmodified Cu_2O -CuO and (b) TiO_2 -modified Cu_2O -CuO photoelectrodes; (c) XRD patterns and (d) visible light (>420 nm) photocurrent generation of unmodified Cu_2O -CuO and TiO_2 -modified Cu_2O -CuO photoelectrodes.

compact underlayer of Cu_2O and a densely packed top layer of CuO nanowires. The growth of CuO nanowires from the bottom of the Cu_2O layer was found to be initiated by thermal treatment.^[17] After modification with TiO_2 , a relatively lower concentration of surface CuO nanowires was observed while the formation of interconnected TiO_2 particles was detected underneath these CuO nanowires. The X-ray diffraction patterns of unmodified Cu_2O -CuO and TiO_2 -modified Cu_2O -CuO photoelectrodes were compared in Fig. 1c. In addition to the peaks assigned to crystalline Cu_2O (36.4° and 42.3°) and CuO (38.7°), a small peak at 25.2° attributed to anatase TiO_2 was observed in the TiO_2 -modified thin film. The Rietveld analysis revealed that the predominant component was Cu_2O ($\sim 50\%$) followed by a small amount of CuO ($\sim 15\%$) and TiO_2 ($\sim 4\%$), and the rest was attributed to the Cu substrate.

Fig. 1d shows the photocurrent generation using unmodified Cu_2O -CuO and TiO_2 -modified Cu_2O -CuO photoelectrodes at -0.36 V vs Ag/AgCl under visible light illumination (>420 nm). When Cu_2O semiconductor was exposed to visible light illumination with energy greater than its band gap, electrons and holes were generated within the semiconductor. Under a negative bias against a Pt counter electrode, electrons were flown from the Pt counter electrode to the Cu_2O working electrode generating a cathodic current. The observed photocathodic current confirmed the p-type behaviour of the Cu_2O electrode.^[18] The unmodified Cu_2O -CuO photoelectrode generated an initial photocurrent density of 1.3 mA/cm^2 but experienced a severe photocurrent decay upon repeating the on-off illumination cycles indicating its photocorrosion, which represents a common issue in Cu_2O -based electrodes. Upon modification with TiO_2 , the initial photocurrent density reached 2.4 mA/cm^2 (which is an 85% photocurrent enhancement). More importantly, the photocurrent profile underwent only a

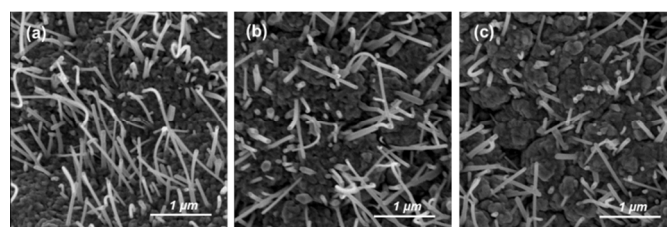


Fig. 2 SEM images of Cu_2O -CuO photoelectrodes modified with precursor of TiO_2 at different duration: (a) 10 min; (b) 30 min; (c) 60 min.

mild decay over the measurement period, with 75% of the initial photocurrent density being retained. With the protective layer of TiO_2 presenting above the Cu_2O surface, the Cu_2O -electrolyte interaction was limited to minimise the problematic direct electron conduction. Additionally, the transfer of photogenerated electrons from Cu_2O to TiO_2 was thermodynamically favoured as the CB of Cu_2O is more negative than that of TiO_2 .^[19] Combining the reduced rate of photocorrosion and the improved charge transfer mechanism, the PEC performance of TiO_2 -modified photoelectrodes was higher and more stable. A similar trend, i.e. increased photocurrent generation and improved photocurrent stability, was also observed when the Cu_2O -CuO photoelectrodes were modified with different concentrations of the TiO_2 precursor

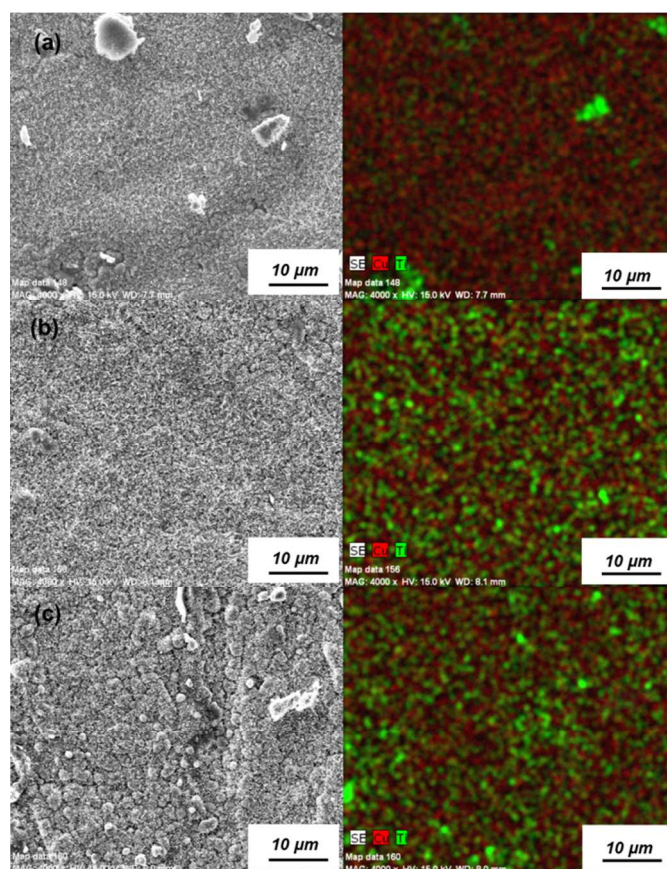


Fig. 3 Energy dispersive X-ray spectroscopy mapping images of Cu_2O -CuO photoelectrodes modified with precursor of TiO_2 at different duration. (a) 10 min; (b) 30 min; (c) 60 min.

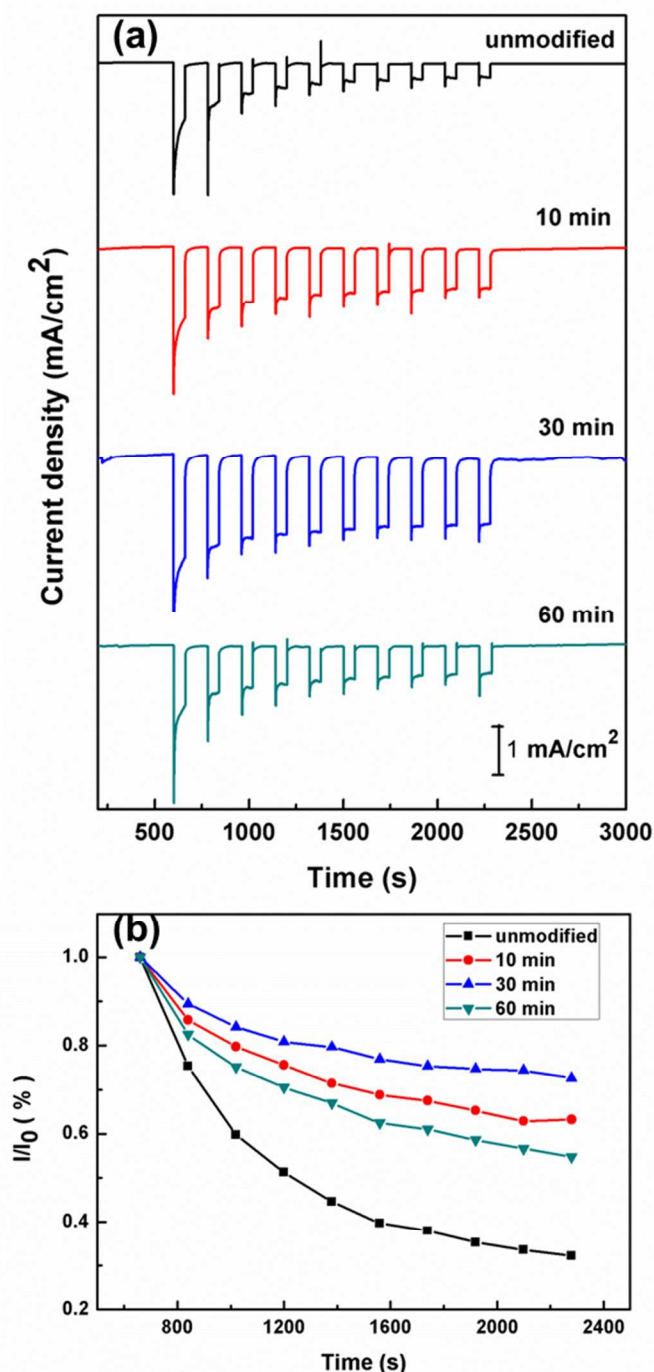


Fig. 4 (a) Visible light (> 420 nm) photocurrent generation and (b) corresponding current decay of $\text{Cu}_2\text{O-CuO}$ photoelectrodes unmodified and modified with precursor of TiO_2 at different duration.

indicating a constructive effect of having a thin TiO_2 protecting layer (please refer to Fig. S1 in supporting information). Another noticeable aspect of the measurements is that the anatase TiO_2 (band gap of 3.2 eV) remained at its ground state without being photoexcited in visible light. Thus, TiO_2 did not contribute an extra electron pool in the photocurrent generation but provided an efficient platform for electron transfer.

As the coverage of TiO_2 on the Cu_2O surface is presumably critical in preventing direct contact with the electrolyte as well as facilitating efficient electron transfer pathways, an investigation on the TiO_2 coating patterns was performed. **Fig. 2** shows the SEM images of $\text{Cu}_2\text{O-CuO}$ photoelectrodes modified with precursor of TiO_2 at different duration. At a short coating time of 10 min, apparent agglomeration of small particles was observed with the CuO nanowires penetrating the surface from the Cu_2O layer underneath. The growth of the agglomerates continued as a longer coating time was applied. For a 60 min photoelectrode coating time, a development of clear grain boundaries (defined as “cracks” between agglomerates) was evident. The grain boundaries significantly influenced the electron transport by introducing defects or charge trap sites for electron-hole recombination, which impeded the shuttling of electrons. In addition, the “cracks” between agglomerates allowed diffusion of the electrolyte to reach the under layer of Cu_2O , thus diminishing the “protective” role of TiO_2 . Elemental mappings of the photoelectrodes over a larger area are presented in **Fig. 3**, where the identity of agglomerates observed in Fig. 2 is verified as TiO_2 (supported by XRD in Fig. 1c). Although at a microscopic level (1 μm scale) the TiO_2 agglomerates appeared to be evenly coated over Cu_2O , the overall coverage of TiO_2 was relatively poor (10 μm scale) as can be seen in the elemental map in Fig. 3a. In contrast, photoelectrodes coated for both 30 min and 60 min showed comparable and considerable TiO_2 coverage on the surface of Cu_2O . The thickness of the 30 min-coated TiO_2 was estimated by back scattered electrons (BSE) imaging to be ca. 140 nm (Fig. S2 in supporting information). The main photoelectrochemical differences between the 30 min and 60 min coating procedures stemmed from the difference in the produced morphological features; photoelectrodes modified for 60 min presented formation of much more severe grain boundaries, which resulted in decreased photocurrent and stability, as will be elaborated below.

As shown in **Fig. 4**, the coating process influences the photocurrent generation and the photoelectrochemical stability of TiO_2 -modified $\text{Cu}_2\text{O-CuO}$ photoelectrodes. In general, our measurements for $\text{Cu}_2\text{O-CuO}$ photoelectrodes modified with an interlayer of TiO_2 revealed two main findings: (1) an increase in the magnitude of the cathodic photocurrent generation, and (2) a slower photocurrent decay over time reflecting the improved stability. As indicated in Fig. 4a, all TiO_2 -modified photoelectrodes demonstrated higher initial photocurrent density upon visible light illumination than that of the unmodified $\text{Cu}_2\text{O-CuO}$ photoelectrode. The initial photocurrent densities were 1.3, 1.6, 2.4 and 1.5 mA/cm^2 for unmodified, 10, 30, and 60 min-modified $\text{Cu}_2\text{O-CuO}$ photoelectrodes, respectively. Photoelectrochemical stability towards self-photodegradation was estimated by monitoring the photocurrent decay over the measurement period (Fig. 4b).^[20] The photoelectrodes prone to the most severe photocorrosion demonstrated the fastest photocurrent decay resulting in low photoactivity at the end of the measurement. The $\text{Cu}_2\text{O-CuO}$

photoelectrode modified with TiO_2 for 30 min showed the highest photocurrent generation and retained 75 % of its initial photoactivity over 40 min of measurement. Even though they

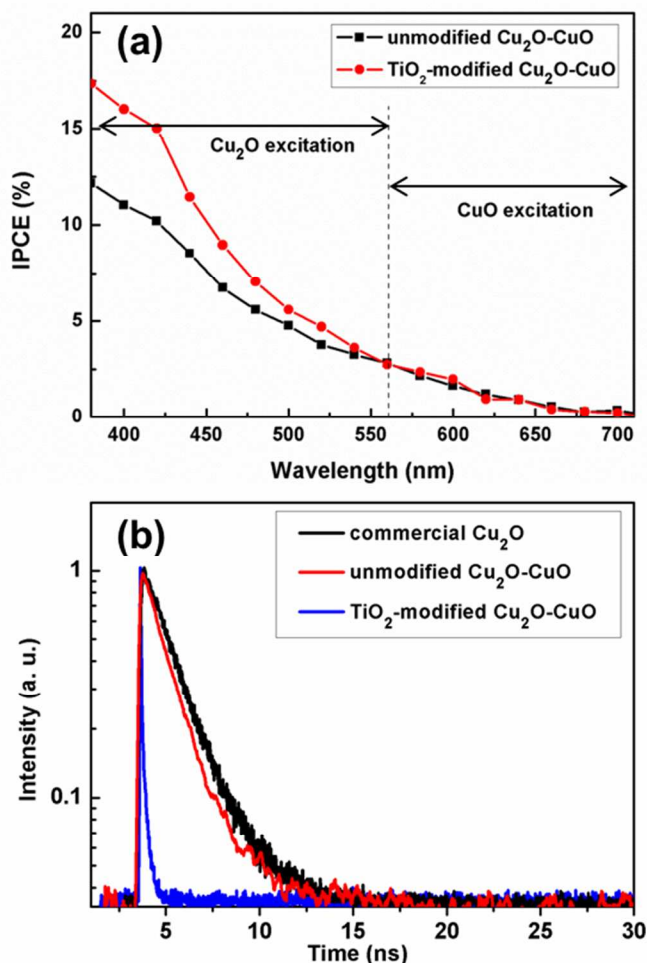


Fig.5 (a) Wavelength-dependent IPCE of unmodified Cu_2O - CuO and TiO_2 -modified Cu_2O - CuO photoelectrodes; (b) Transient decay curves of commercial Cu_2O , unmodified Cu_2O - CuO and TiO_2 -modified Cu_2O - CuO photoelectrodes.

performed better than unmodified Cu_2O - CuO photoelectrode, the photoelectrodes modified for 10 and 60 min, were inferior in both aspects. As the conduction band of TiO_2 lies lower than that of Cu_2O , the presence of a TiO_2 layer on top of Cu_2O created a thermodynamically feasible pathway to shuttle the electrons photogenerated in Cu_2O . The creation of a junction between TiO_2 and CuO facilitates charge transfer, thus improving the overall photocurrent generation. In accordance with the TiO_2 coverage and agglomeration states shown in Fig. 2 and Fig. 3, the Cu_2O - CuO photoelectrode modified with TiO_2 for 30 min revealed the most optimal TiO_2 coverage with small dispersed aggregates that provided the most “protective” and surface passivating function for Cu_2O . Samples with low coverage (modified for 10 min) and a large amount of cracks between large agglomerates (modified for 60 min) showed relatively ineffective surface passivation. They only retained 65 % (modified for 10 min) and 56 % (modified for 60 min) of

their initial activity, respectively. Another possible reason for lower photoactivity and stability observed in Cu_2O - CuO photoelectrode modified for 60 min is the trapping of electrons in the long lived Ti^{3+} states (please refer to XPS data in Fig. S2 in supporting information).^[12, 21, 22] Upon generation in Cu_2O , the electrons are efficiently transferred to TiO_2 . Instead of further injection into CuO or electrolyte, the electrons are possibly reducing Ti^{4+} to Ti^{3+} resulting in lower photoactivity. Wavelength-dependent photocurrent analysis was performed to measure the incident photon-to-current efficiency of the Cu_2O - CuO photoelectrodes (Fig. 5a). As expected, the overall conversion efficiency was higher in TiO_2 -modified Cu_2O - CuO photoelectrodes. Interestingly, the photocurrent enhancement in TiO_2 -modified Cu_2O - CuO photoelectrodes was only observed at the wavelengths shorter than 560 nm, which corresponds to the optical band gap of Cu_2O (~2.2 eV). This result supports the earlier suggestion on the charge transfer from the conduction band of Cu_2O to TiO_2 . As charge recombination is suppressed, higher utilisation rate of electrons is achieved in the wavelength region where Cu_2O is excited. The photoactivity in wavelengths longer than 560 nm appeared as the tailing off in the overall photocurrent profile and likely originated from the narrower band gap CuO component in the photoelectrode. Since the electron transfer from CuO to TiO_2 is prohibited as the conduction band of CuO is more positive than that of TiO_2 ,^[23] the presence of TiO_2 does not influence the conversion efficiency in this wavelength region. CuO nanowires offer an energetically favourable electron transfer pathway for the electrons originated from Cu_2O and TiO_2 .

Fluorescence lifetimes of commercial Cu_2O , unmodified Cu_2O - CuO and TiO_2 -modified Cu_2O - CuO photoelectrodes were measured using the time-correlated single photon counting technique (Fig. 5b). Samples were excited at 405 nm and monitored at 510 nm. The decay constants were determined using bi-exponential analysis as shown in equation (1), from

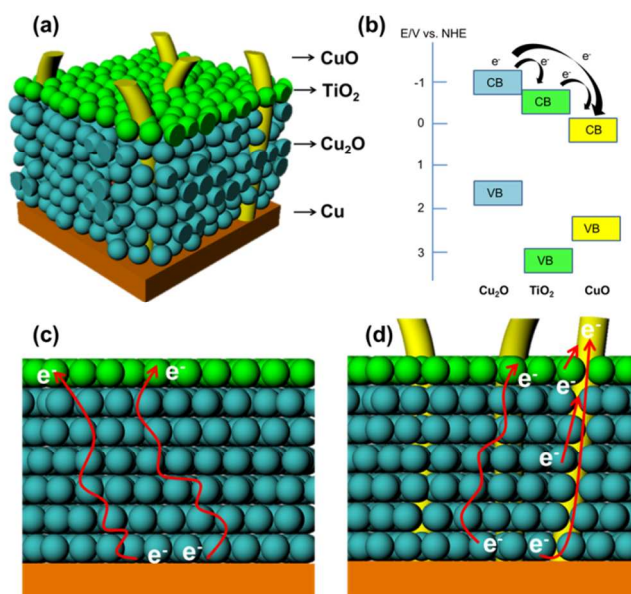


Fig. 6 Schematic illustration of (a) TiO₂-modified Cu₂O-CuO photoelectrodes; (b) corresponding energy band positions; electron diffuse transfer from Cu₂O to interface (c) without one-dimensional CuO nanowires and (d) with one-dimensional CuO nanowires.

which average lifetimes were obtained using equation (2).

$$y = A_1 \exp(-t / \tau_1) + A_2 \exp(-t / \tau_2) \quad (1)$$

$$\langle \tau \rangle = (A_1 \tau_1 + A_2 \tau_2) / (A_1 + A_2) \quad (2)$$

where A₁ and A₂ are the corresponding amplitudes of the fast decay component (τ₁) and slow decay component (τ₂). Note that the TiO₂ component was not excited at this wavelength and therefore, the observed fluorescence originated from Cu₂O. The average excited state lifetime (τ) for commercial Cu₂O (commercial Cu₂O powder spin-coated on Cu foil) was 1.72 ns. In the unmodified Cu₂O-CuO photoelectrodes, a slightly shorter decay process of 1.40 ns suggested that the quenching of excitation in Cu₂O was affected slightly due to the electron transfer to CuO nanowires. Even though an additional charge relaxation pathway was generated by the presence of CuO nanowires, its effect was not obvious probably due to its low degree. The TiO₂-modified Cu₂O-CuO photoelectrode showed the shortest τ of ~ 0.2 ns. Attributed to good coverage and close proximity of TiO₂ to the Cu₂O layer as revealed by the SEM technique, the photoexcited electrons in Cu₂O were transferred to TiO₂ efficiently instead of relaxing back to the ground state with radiative emission. As a result of this favourable charge transfer in Cu₂O, the photoexcited electron consumption (photocurrent generation) was boosted as demonstrated by IPCE and PEC analyses.

Conclusions

In summary, we have demonstrated a beneficial impact of coating a thin layer of TiO₂ on an anodised Cu₂O photoelectrode on its visible light photoelectrochemical performance. Two noticeable improvements were observed: enhanced magnitude of the photocurrent generation and improved photoelectrochemical stability of Cu₂O. The increased stability is especially significant as self-photodegradation of Cu₂O has been the most challenging aspect of this unstable p-type material for years. **Fig. 6** illustrates the schematic configuration of the TiO₂-modified Cu₂O-CuO photoelectrode prepared in this work. Based on the experimental results obtained, the photoelectrochemical properties are proposed to be enhanced through: (1) Cu₂O surface passivation by TiO₂, preventing redox reactions at the Cu₂O-electrolyte interface; and (2) improved charge transport channels attributed to the well-aligned band gap structure, in which the photoexcited electrons in Cu₂O are thermodynamically transferred to TiO₂ or CuO nanowires or from Cu₂O to TiO₂ and subsequently CuO nanowires. The embedment of one-dimensional CuO nanowires underneath the Cu₂O layer also improved the physical stability of the well-designed Cu₂O-TiO₂-CuO heterojunction thin film. Instead of the electron transfer by random diffusion from Cu₂O to the interface, the embedment of one-dimensional CuO nanowires

provided a fast and direct electron transfer pathway. Although a complete inhibition of the photoactivity decay was not achieved at this stage, this work opens immense possibilities for improvement by further optimisation of the process.

Acknowledgements

This work was financially supported by the Australia Research Council Discovery Project (DP 110101638). The authors would like to acknowledge the UNSW Mark Wainwright Analytical Centre for providing facility and technical supports. Dr. Bill Gong from Solid State & Elemental Analysis Unit of UNSW is gratefully acknowledged for his help in XPS measurement and analysis. The authors thank Carlos G. Morales-Guio and Prof. Xile Hu from École Polytechnique Fédérale de Lausanne (EPFL) for assistance in the back scattered electron (BSE) imaging.

Author contributions

P. W. fabricated the photoelectrodes, conducted SEM, EDS, XRD, PEC and IPCE measurements. Dr. B. G. conducted XPS experiment and analysis. Dr. X.M. W. conducted TCSPC measurement and analysed data. Prof. R. A. and Dr. Y.H. N. supervised this work. All authors analysed the data and completed the paper.

Notes and references

^aParticles and Catalysis Research Group, School of Chemical Engineering, The University of New South Wales, Sydney, NSW 2052, Australia. E-mail: yh.ng@unsw.edu.au; r.amal@unsw.edu.au

^bSchool of Photovoltaics and Renewable Energy Engineering, The University of New South Wales, Sydney, NSW 2052, Australia

†Electronic Supplementary Information (ESI) available: [details of any supplementary information available should be included here]. See DOI: 10.1039/b000000x/

1. S. Trasatti, *J. Electroanal. Chem.*, 1999, **476**, 90-91.
2. R. Abe, *J. Photochem. Photobio. C - Rev.*, 2010, **11**, 179-209.
3. A. Fujishima and K. Honda, *Nature*, 1972, **238**, 37-38.
4. C. Ng, A. Iwase, Y. H. Ng and R. Amal, *ChemSusChem*, 2013, **6**, 291-298.
5. Y. H. Ng, A. Iwase, A. Kudo and R. Amal, *J. Phys. Chem. Lett.*, 2010, **1**, 2607-2612.
6. O. Khaselev and J. A. Turner, *J. Electrochem. Soc.*, 1998, **145**, 3335-3339.
7. C. G. Morales-Guio, S. D. Tilley, H. Vrubel, M. Grätzel and X. Hu, *Nature Commun.*, 2014, **5**, 3059.
8. L. J. Minggu, W. R. Wan Daud and M. B. Kassim, *Int. J. Hydrogen Energy*, 2010, **35**, 5233-5244.
9. A. J. Nozik and R. Memming, *J. Phys. Chem.*, 1996, **100**, 13061-13078.
10. A. J. Nozik, *Appl. Phys. Lett.*, 1977, **30**, 567-569.
11. Y. Li and J. Zhang, *Laser Photon. Rev.*, 2010, **4**, 517-528.

12. A. Paracchino, V. Laporte, K. Sivula, M. Grätzel and E. Thimsen, *Nature Mater.*, 2011, **10**, 456-461.
13. K. Sun, N. Park, Z. Sun, J. Zhou, J. Wang, X. Pang, S. Shen, S. Y. Noh, Y. Jing, S. Jin, P. K. L. Yu and D. Wang, *Energy Environ. Sci.*, 2012, **5**, 7872-7877.
14. Y. V. Pleskov, A. M. Kraitsberg, G. Y. Kolbasov, N. I. Taranenko and V. G. Lipyavka, *Sol. Energy Mater.*, 1991, **22**, 119-126.
15. Z. Zhang and P. Wang, *J. Mater. Chem.*, 2012, **22**, 2456-2464.
16. P. Wang, Y. H. Ng and R. Amal, *Nanoscale*, 2013, **5**, 2952-2958.
17. S. L. Shinde and K. K. Nanda, *RSC Adv.*, 2012, **2**, 3647-3650.
18. P. E. de Jongh, D. Vanmaekelbergh and J. J. Kelly, *J. Electrochem. Soc.*, 2000, **147**, 486-489.
19. W. Siripala, A. Ivanovskaya, T. F. Jaramillo, S. H. Baeck and E. W. McFarland, *Sol. Energy Mater. Sol. Cells*, 2003, **77**, 229-237.
20. N. J. Bell, Y. H. Ng, A. Du, H. Coster, S. C. Smith and R. Amal, *J. Phys. Chem. C*, 2011, **115**, 6004-6009.
21. J. P. Yasomanee and J. Bandara, *Sol. Energy Mater. Sol. Cells*, 2008, **92**, 348-352.
22. L. B. Xiong, J. L. Li, B. Yang and Y. Yu, *J. Nanomater.*, 2012, 2012.
23. J. Bandara, C. P. K. Udawatta and C. S. K. Rajapakse, *Photochem. Photobiol. Sci.*, 2005, **4**, 857-861.